FEBS Letters 504 (2001) 212–218 FEBS 25157

Research Letter

Molecular dynamics study of aquaporin-1 water channel in a lipid bilayer

Fangqiang Zhu, Emad Tajkhorshid, Klaus Schulten*

Beckman Institute, University of Illinois at Urbana-Champaign, 405 N. Mathews, Urbana, IL 61801, USA

Received 11 July 2001; accepted 23 July 2001

First published online 7 August 2001

Edited by Andreas Engel and Giorgio Semenza

Abstract The aquaporin-1 water channel was modeled in a palmitoyl-oleoyl-phosphatidyl-choline lipid bilayer, by means of molecular dynamics simulations. Interaction of the protein with the membrane and inter-monomer interactions were analyzed. Structural features of the channel important for its biological function, including the Asn-Pro-Ala (NPA) motifs, and the diffusion of water molecules into the channels, were investigated. Simulations revealed the formation of single file water inside the channels for certain relative positions of the NPA motifs.

Key words: Aquaporin; Molecular dynamics; Water conduction; Asn-Pro-Ala motif; Channel structure; Aquaporin-1

1. Introduction

Aquaporins (AQPs) are a family of membrane channel proteins that can be found in a wide range of species, including human and other mammalians, amphibia, insects, plants, and bacteria (for a recent review, see [1]). AQPs are responsible for the high osmotic permeability of certain cell membranes, such as mammalian red cell membranes [2–4]. All of the members of this family conduct water across the membrane to various degrees, and some of them can also conduct different solutes, such as glycerol and other small monosaccharides [1,5]. The amino acid sequence of all AQPs is a tandem repeat, i.e., the first and second halves of the protein involve very similar sequences. AQPs also exhibit a structural pseudo two-fold symmetry, resulting from the similarity of the sequence of the two repeats [5–8]. Common to all AQPs is a characteristic NPA (Asn-Pro-Ala) motif in each repeat [9,10]. Structurally, AQPs fold into six trans-membrane and two short helices. These short helices, which start from the middle of the membrane and go outward to the membrane surface, are preceded by two loops folding into the membrane from the surface. The NPA motifs are located near the N-termini of the short helices, almost in the middle of the membrane.

AQPs play important physiological roles, and thereby are of considerable importance in the biomedical sciences. Because of the variety of functions of these channels in animals, they have been associated with several clinical disorders [3]. AQPs are even more important in plants where they play a key role in several different processes [11]. More than 30 different AQPs have been characterized in different microorganisms [12].

Aquaporin-1 (AQP1) was the first identified member of the family [13–15]. It is present in multiple human tissues, such as red blood cells and renal proximal tubules. AQP1 forms a homotetrameric assembly in lipid membranes [16,17]. Many studies, however, have indicated that each monomer is a functional channel [18–21]. AQP1 has a relatively high water permeability (about two water molecules/monomer/ns [14,22]), but it does not conduct ions or other solutes [15,23]. In particular, AQP1 does not exhibit proton conduction, which is an interesting feature because protons can usually pass along a column of water without significant moves of heavy atoms.

Several AQP1 structures at increasing levels of resolution have been solved using membrane crystals purified from red cells [7,8,24–28]. We used the structure with the highest resolution [7] to construct a model of AQP1 in a lipid bilayer. This structure provided us with sufficient structural information needed for studying AQP1 at the atomic level. Here we report the results of an extensive series of molecular dynamics (MD) simulations performed on a fully hydrated model of the AQP1 tetramer in the lipid bilayer.

2. Materials and methods

The crystal structure of AQP1 [7] was obtained from the Protein Data Bank (PDB entry 1FQY). The monomeric coordinates were replicated using the transformation matrices provided in the PDB file, in order to form a tetrameric structure. Hydrogen atoms were then added to the protein using XPLOR [29], and employing the default titration states for titratable amino acids.

The available crystal structure [7] does not resolve any water molecules. For internal hydration of the structure, the program DOWSER [30] was used. The program checks a protein structure to locate internal cavities and accounts for the hydrophilicity of these cavities in

*Corresponding author. Fax: (1)-217-244 6078.
E-mail address: kschulte@ks.uiuc.edu (K. Schulten).

Abbreviations: AQP, aquaporin; POPC, palmitoyl-oleoyl-phosphatidyl-choline; NPA, Asn-Pro-Ala; AQP1, aquaporin-1; RMSD, root mean square deviation; PME, Particle Mesh Ewald; GlpF, glycerol facilitator; MD, molecular dynamics

PII: S0014-5793(01)02749-1

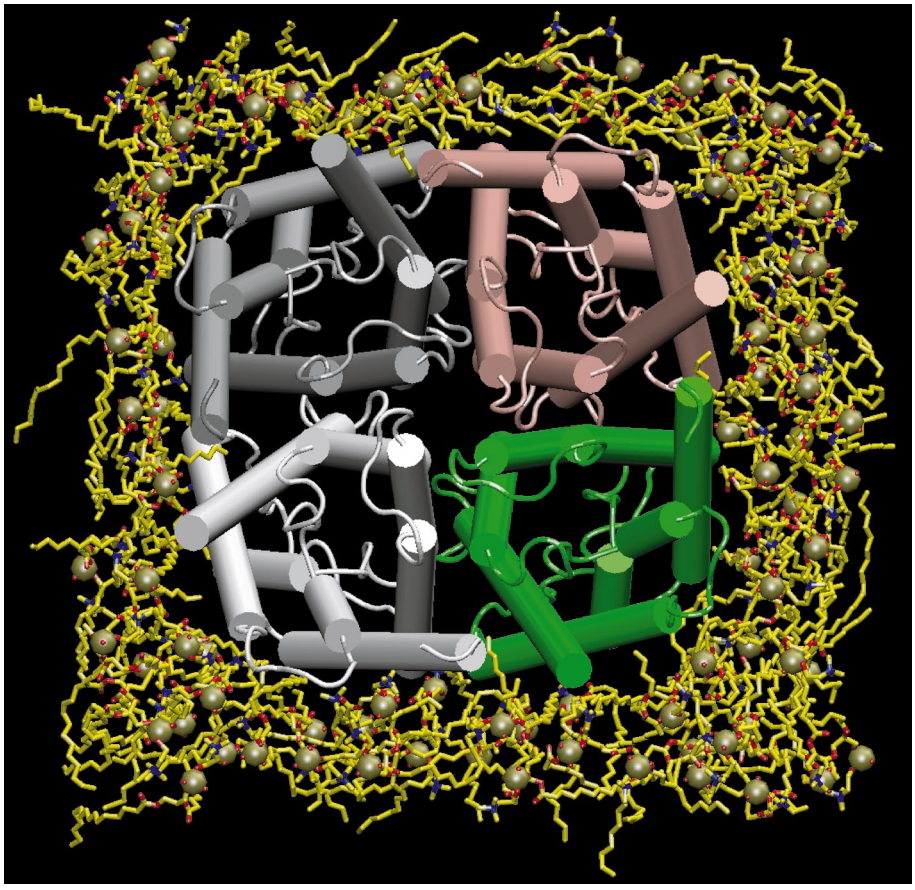

Fig. 1. Lipid configurations at the end of a 1 ns equilibration step, during which the coordinates of the protein were fixed (phase I). The protein is shown in cartoon representation, lipids in licorice representation (hydrogen atoms not shown); phosphorus atoms of lipids are drawn as VDW spheres (view from the cytoplasmic side). Water molecules of the system are not shown in this view.

terms of the energy of interaction of a water molecule with the surrounding atoms. Further water molecules were placed in the channel using the program SOLVATE [31].

The hydrated tetramer was then superimposed on a solvated palmitoyl-oleoyl-phosphatidyl-choline (POPC) lipid bilayer patch consisting of 200 lipids, which had been equilibrated in our previous studies [32,33] at 1 atm and 340 K for 1 ns, using full electrostatics, periodic boundary conditions, and a flexible unit cell. The membrane patch was sufficiently large to accommodate the tetrameric structure of AQP1. The majority of the lipids overlapping with the protein were removed. In some cases, however, modification of the conformation of lipids could remove bad contacts, thereby avoiding the introduction of large gaps around the protein. This was done using programs VMD [34] and Insight-II [35]. More water was included in the system by adding a 30 Å thick slab from an equilibrated water box. The resulting system contained about 60 000 atoms.

Most simulations were performed in two phases. In a first phase, the lipids and bulk water were minimized and equilibrated for 1 ns while keeping the coordinates of protein atoms fixed. In a second phase, the protein was free to move, and minimization and equilibration steps were repeated for the whole system. In the following sections, the phases will be referred to as phases I and II, respectively. All simulations were performed using the CHARMM22 force field [36,37], the TIP3P water model and the MD program NAMD2 [38], with periodic boundary conditions at constant temperature (310 K) and constant pressure of 1 atm (NpT ensemble). Langevin dynamics and Langevin piston methods were used to keep temperature and pressure constant. Full electrostatics was employed using the Particle Mesh Ewald (PME) method [39]. In order to render the whole system electrically neutral, as required by the PME method, eight chloride ions were added to the bulk water of the unit cell. A 1 ns simulation of the fully hydrated model of AQP in the lipid bilayer took about 5 days of parallel computation on 64 Cray T3E processors.

3. Results and discussion

Several models were constructed and simulated. In the first model (model 1) the channels included at the beginning of the simulation only water molecules added by DOWSER [30]. In model 2, additional water molecules were included by SOLVATE [31], in an attempt to form a continuous water file in the channel. In model 3, the NPA motifs were arranged at the outset of the simulation to adopt the hydrogen bond network observed in the glycerol facilitator (GlpF) structure [5]. Model 4 had the same starting structure as model 3, but was subjected to MD simulations with application of constraints on the NPA motifs. These modifications and constraints were applied to preserve the relative position of the NPA motifs, a feature which was found unstable in the absence of such interventions.

3.1. Protein/lipid behavior

Figs. 1 and 2 show the top and side views of the system at the end of the 1 ns equilibration of lipids and bulk water (phase I). During the simulations, lipid molecules adopt conformations that match the shape and charges of the exposed surface of the protein. During the equilibration of the lipids the thickness of the lipid bilayer (measured by average vertical distance between the phosphorus atoms of lipids in the two leaflets) also changes. Fig. 3 shows the evolution of the membrane thickness during the 2 ns of equilibration (phases I and

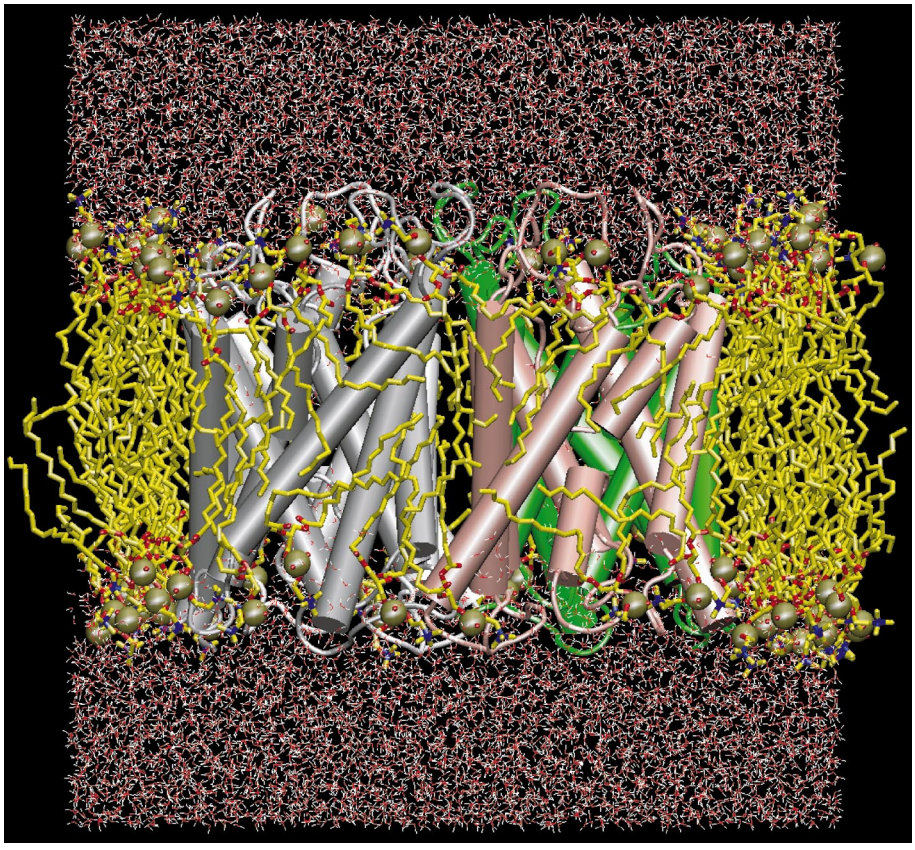

Fig. 2. Side view of the system in Fig. 1. Water molecules are shown.

II). One can discern an increase in the thickness of the membrane which is mainly due to the relaxation of the lipids at the protein–lipid interface. In phase II of the simulation, the change of lipid thickness is relatively small (less than 2 Å), implying that the lipids had reached a structural equilibrium with the protein.

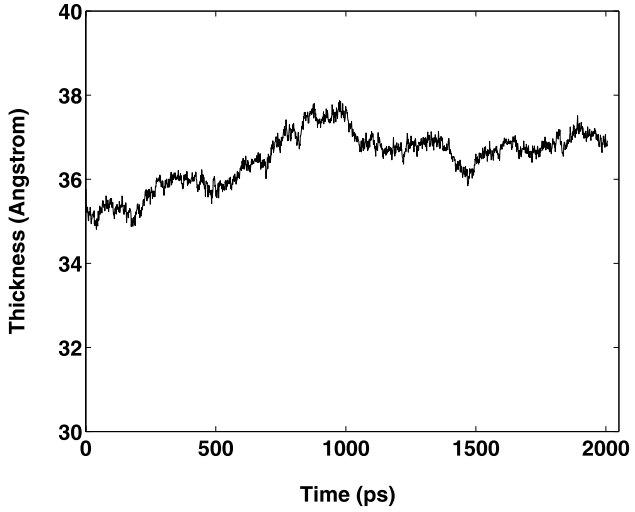

Fig. 3. Thickness of the lipid bilayer during a 2 ns simulation. The protein was fixed during the first nanosecond (phase I). The thickness was calculated as the difference between the average z coordinates (membrane plane normal to the z axis) of the lipid phosphorus atoms in each leaflet.

The protein exhibited significant fluctuation during the simulations. This is demonstrated in Fig. 4 where the root mean square deviation (RMSD) of the structure of one of the AQP1 monomers relative to the crystal structure is plotted as a function of equilibration time. The RMSD of C_α atoms is within bounds typical for MD simulations of structurally

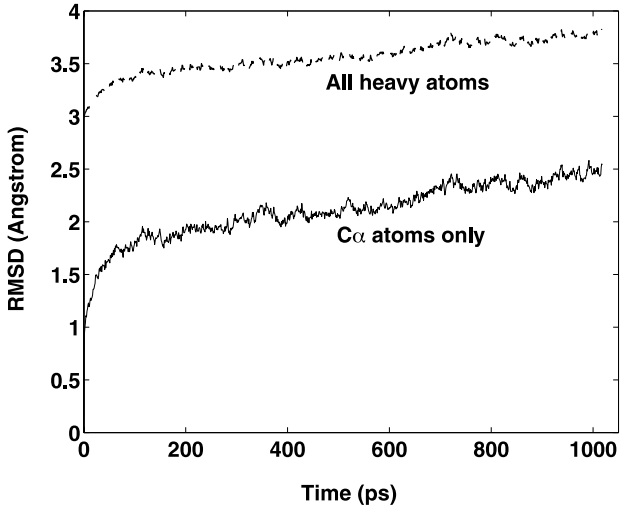

Fig. 4. RMSD of one of the AQP1 monomers during the 1 ns equilibration (phase II). Every frame from the simulation was first aligned with respect to the crystal structure of the AQP1 monomer, then the RMSD was calculated. The dashed line shows the RMSD values for all non-hydrogen atoms of the monomer, and the solid line only the RMSD values of C_α atoms.

known and stable proteins; the side chains show untypically large fluctuations. This may be attributed to the relatively low resolution of the starting structure (3.8 Å in plane, 4.4 Å normal to plane); while the overall folding of the protein has been described properly in the crystal structure, structural information about the side chains, especially in regard to the interactions between the amino acids, may not yet be accurate. This issue will be discussed further below where the NPA motif is described. The RMSD between the C_α atoms of any two monomers at the end of the equilibration ranges from 2.1 Å to 2.6 Å (data not shown), values which are comparable to the RMSD between a monomer and the crystal structure.

Several major interactions between the amino acids and the head groups of lipids were observed in AQP1 monomers. The positively charged side chains of Lys_8, Arg_{12}, Arg_{93}, and Arg_{126} establish salt bridges with the negatively charged lipid phosphate groups. Furthermore, several amino acids form hydrogen bonds with lipids. Among these are Trp_{11}, Ser_{86}, Ser_{117}, Ser_{135}, Gly_{136}, Asn_{205} and Ser_{207}. As expected these amino acids are mainly located in the loop regions of the protein.

Analyzing the major electrostatic interactions between the neighboring monomers in 1 ns showed that Arg_{12} and Asp_{228}, which are located near the N- and C-termini in neighboring monomers, stabilize the tetrameric assembly. Another pronounced interaction was found to arise through a hydrogen bond between the Gly_{30} backbone oxygen and the hydroxyl group of Tyr_{186} in the neighboring monomer. Within the same monomer, His_{74} formed a hydrogen bond with the conserved Glu_{17}; a salt bridge between Glu_{142} and Arg_{195} proved very stable during all the simulations.

3.2. Water arrangement in the channel

In model 1, only two water molecules added by DOWSER were present in the channel at the beginning of the simulations. These water molecules were completely isolated from the bulk water. After 1 ns of equilibration several water molecules diffused from the bulk into the channels. However, only in one channel did we observe a formation of an almost continuous single file of water molecules; in all other channels the water chain was not well established.

The AQP1 channel has a high water permeability, and one can expect the presence of a continuous water column inside the channel. An empty channel is very unlikely to exist. Keeping this in mind, we decided to repeat our calculations in a model in which the water pores were completely hydrated (model 2). This was accomplished using the program SOLVATE that suggested more hydration sites inside the channels than the program DOWSER.

During phase I of the simulation of model 2, the water molecules inside the channels rearranged themselves very quickly, and formed a single file, where each water molecule was H-bonded to the adjacent molecule(s). Fig. 5 shows the water arrangement in one of the channels at the end of this phase. In phase II when the protein was free to move, however, the water file was disturbed by protein fluctuations (see Fig. 4), and was often disconnected. As we will discuss in Section 3.3, this was mainly due to the large conformational changes of side chains, especially the Asn residues of the NPA motifs.

The major hydrogen bond partners of the water molecules inside the channel are the side chain nitrogen atoms of the Asn residues in the NPA motifs, as well as the main chain hydrogen (HN) and oxygen atoms of the two loops preceding the NPAs in each half. The free sulfhydryl group of Cys_{189} was found to be mainly pointing toward the channel during the simulations. This is in accordance with the fact that binding of a mercury atom to this residue blocks the channel.

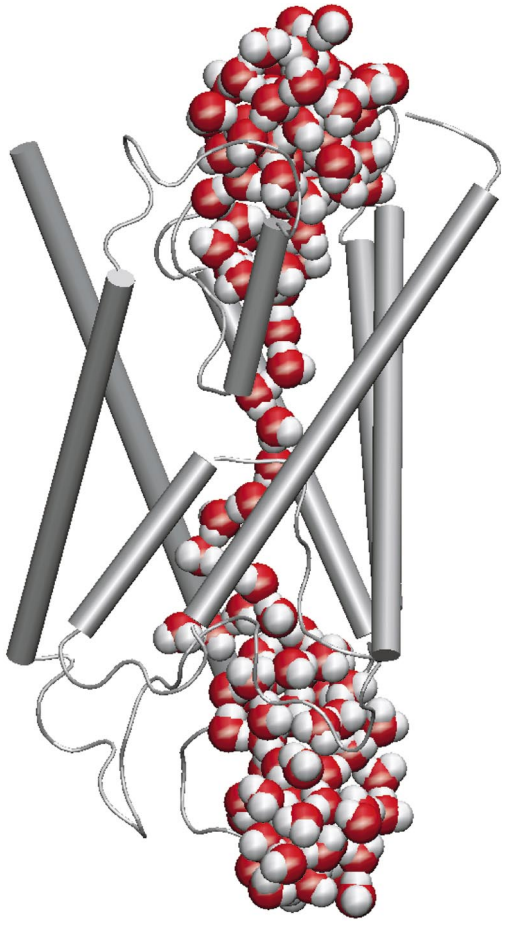

Fig. 5. Snapshot of water molecules inside the channel at the end of the 1 ns equilibration (phase I) in which the protein was fixed.

It has been suggested that the central channel formed by the tetramerization of AQP1 could conduct water or ions [1,5]. In none of the models studied in the present work, however, did we observe diffusion of bulk water into the central channel. This is consistent with the hydrophobic nature of the major part of the surface of the central channel.

3.3. The structure of NPA motifs

The NPA motifs are highly conserved in all AQPs, and are thus expected to play an important role in the function of the channel. Our simulations of models 1 and 2 clearly showed that the side chains of Asn_{76} and Asn_{192} in the NPA motifs are not stable. In fact, the side chains flip away from their original positions soon after the removal of the constraints on the protein in phase II of the simulations. These large fluctuations resulted in most cases in the rupture of water files that form in the four channels. The ruptures are caused mainly through the introduction of a large spatial gap between the Asn residues of the two NPA motifs. The perturbed config-

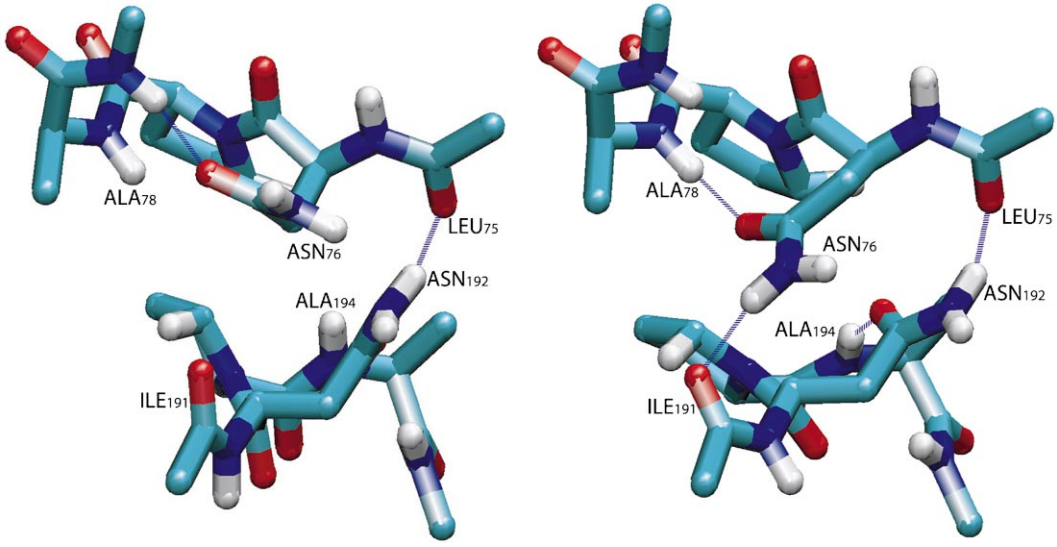

Fig. 6. Modification of the NPA motif; left: NPA motif from AQP1 crystal structure (1FQY); right: NPA motif after modification (models 3 and 4). In this structure, four hydrogen bonds (two between Asn residues and backbone nitrogen atoms of Ala residues in the same repeat, and two between Asn residues and backbone carbonyl oxygens of the other repeat) are well established. These hydrogen bonds are symmetric with respect to the tandem repeat. This configuration is very similar to that of the NPA motif in the GlpF structure [5].

uration of the Asn residues, unfavorable for the conduction of water, is inconsistent with the high water permeability of AQP1. One explanation for this perturbation might be structural inaccuracies of the NPA motifs in the published crystal structure. In regard to this, it is noteworthy that calculations on another member of the family, namely GlpF (paper submitted), found a stable configuration of the NPA motifs for this protein. The calculations were performed on the structure of GlpF solved at a higher resolution (2.2 Å) [5]. In this structure, the side chains of each Asn from the NPA motifs are H-bonded to the Ala backbone nitrogen of the same repeat and the backbone carbonyl oxygen of the residue preceding the Asn in the other repeat. These interactions effectively constrain the orientation of the Asn side chain, and make a polar hydrogen from the side chain NH group point toward the channel, serving as an important hydrogen bond donor for the glycerol or water molecules in the channel.

Since the NPA motifs are conserved for the whole family of AQPs, we believe that they should have similar structural and functional features in AQP1 and GlpF; in particular, the Asn residues of the motifs in AQP1 should be stable and play a similar role in the water permeation. Therefore, we decided to modify the NPA motifs of AQP1 according to the GlpF structure. Fig. 6 shows the original configuration of the NPA motifs and the configuration after the modification. In the original structure, some hydrogen bonds are not formed, especially the one between the side chain of Asn_{76} and the backbone carbonyl oxygen of Ile_{191}. The modified structure (model 3) has the same set of hydrogen bonds as in the GlpF structure. The structural changes needed for such manipulations were minimal and well within the resolution of the crystal structure; the applied modifications only precluded the possibility of initially establishing hydrogen bonds to the other sites in that region.

After applying the modifications, the Asn side chains were found significantly more stable, mainly due to the hydrogen bonds described above. Furthermore, the water molecules inside the channels were also better ordered than before, indicating that such structural modifications are reasonable. In our simulations, the hydrogen bonds between residues in the same repeat (Asn and Ala) were fairly stable at all times; but the cross-repeat hydrogen bonds (between Asn and a backbone oxygen of the other repeat) were still more vulnerable to disturbance than found in GlpF simulations (paper submitted), and some of the hydrogen bonds were broken in the first 100 ps of the simulations. Examination of the trajectories showed that there are other structural features in GlpF that stabilize the peculiar NPA motifs and are absent in the AQP1 structure. Furthermore, different positions of other amino acids, such as Arg_{195}, result in different hydrogen bond networks in the channel of GlpF and AQP1.

The hydrogen bonds between the NPA motifs are sensitive to their relative positions. Because of large fluctuation of the structure especially at the beginning of the simulations, in model 4, we applied constraints on the two cross-repeat hydrogen bonds in each monomer, in order to keep the bonds formed. As expected, forcing the NPA motifs to stay close to each other further improved the tendencies of water molecules in the channels to form continuous water files, as was observed in three monomers.

The available structures of AQP1 [7,8] do not agree with respect to the position of several key amino acids, including the NPA motifs. They also disagree in some respect with the high resolution (2.2 Å) GlpF structure [5]. Comparison of the structure and the results of simulations performed on GlpF and AQP1 suggests that an improved AQP1 structure is needed for completely unraveling the mechanism of water transport in AQP1.

For instance, in the crystal structure of AQP1 [7], Arg_{195} forms a salt bridge with Glu_{142}, which is very stable in all simulations. This keeps the side chain of Arg_{195} away from the interior of the water channel. The corresponding residue in GlpF, Arg_{206}, has a very different orientation, and by directly interacting with water and solutes plays an important

role in the conduction mechanism. We note that this Arg is one of the highly conserved residues in the whole AQP family. In the AQP1 structure resolved by Mitra et al. [8], the orientation of this Arg, which is also one of the residues lining the channel, is more similar to that in GlpF. It is likely that the assignment of its side chain in the structure we used (1FQY) is not accurate. Furthermore, in the loops preceding the NPA motifs in the GlpF structure, glycerol and water molecules form hydrogen bonds exclusively with main chain carbonyl oxygens; whereas in AQP1, some main chain HN atoms also contribute. This could be either an intrinsic difference between these two homologs, or may be an artifact due to the limited resolution of the AQP1 structure. Ongoing crystallographic studies to improve the resolution of the structure of AQP1 [40] may shed light on the issue.

4. Conclusion

The structure and dynamics of the AQP1 water channel in a lipid bilayer have been studied using MD simulations. The protein model was constructed based on one of the highest resolution AQP1 structures that for the first time permitted exploring AQP1 function at an atomic level. The complete model comprises a tetrameric AQP1 embedded in a fully hydrated POPC lipid bilayer, including altogether 60 000 atoms. Several interactions between the monomers as well as between the protein and lipids have been characterized. The calculations revealed a spontaneous diffusion of water molecules from the bulk into the interior parts of the channel and demonstrated in some cases the formation of continuous water files inside the monomers. The central channel formed by the tetramer was not hydrated at any time during the simulation and, therefore, does not seem to be involved in any ion or water conduction. Although the overall structure of the protein was relatively stable during the simulations and several functionally significant features of the channel could be inferred from the simulations, the details of the position of side chains and interactions between key groups in the channel do not seem to be consistently described in the available structures of AQP1, and further crystallographic analyses and simulations with the improved structure are required.

Acknowledgements: Our work was supported by the National Institute of Health, Grants PHS 5 P41 RR05969 and R01 GM60946. The authors also acknowledge the computer time provided by the Grant NRAC:MCA93S028. The figures in this paper were created with the molecular graphics program VMD [34].

References

[1] Borgnia, M., Nielsen, S., Engel, A. and Agre, P. (1999) Annu. Rev. Biochem. 68, 425–458.
[2] Agre, P., Brown, D. and Nielsen, S. (1995) Curr. Opin. Cell Biol. 7, 472–483.
[3] Agre, P., Bonhivers, M. and Borgnia, M.J. (1998) J. Biol. Chem. 273, 14659–14662.
[4] Verkman, A., Hoek, A.V., Ma, T., Frigeri, A., Skach, W., Mitra, A., Tamarappoo, B. and Farinas, J. (1996) Am. J. Physiol. Cell Physiol. 39, C12–C30.
[5] Fu, D., Libson, A., Miercke, L.J.W., Weitzman, C., Nollert, P., Krucinski, J. and Stroud, R.M. (2000) Science 290, 481–486.
[6] Calamita, G. (2000) Mol. Microbiol. 37, 254–262.
[7] Murata, K., Mitsuoka, K., Hirai, T., Walz, T., Agre, P., Heymann, J.B., Engel, A. and Fujiyoshi, Y. (2000) Nature 407, 599–605.
[8] Ren, G., Reddy, V.S., Cheng, A., Melnyk, P. and Mitra, A.K. (2001) Proc. Natl. Acad. Sci. USA 98, 1398–1403.
[9] Wistow, G., Pisano, M. and Chepelinsky, A. (1991) Trends Biochem. Sci. 16, 170–171.
[10] Pao, G., Wu, L., Johnson, K., Hofte, H. and Chrispeels, M. (1991) Mol. Microbiol. 5, 33–37.
[11] Johansson, I., Karlsson, M., Johanson, U., Larsson, C. and Kjellbom, P. (2000) Biochim. Biophys. Acta 1465, 324–342.
[12] Hohmann, S., Bill, R.M., Kayingo, G. and Prior, B.A. (2000) Trends Microbiol. 8, 33–38.
[13] Preston, G.M. and Agre, P. (1991) Proc. Natl. Acad. Sci. USA 88, 11110–11114.
[14] Zeidel, M.L., Ambudkar, S.V., Smith, B.L. and Agre, P. (1992) Biochemistry 31, 7436–7440.
[15] van Hoek, A.N. and Verkman, A.S. (1992) J. Biol. Chem. 267, 18267–18269.
[16] Verbavatz, J.M., Brown, D., Sabolic, I., Valenti, G., Ausiello, D.A., van Hoek, A.N., Ma, T. and Verkman, A.S. (1993) J. Cell Biol. 123, 605–618.
[17] Walz, T., Smith, B.L., Zeidel, M.L., Engel, A. and Agre, P. (1994) J. Biol. Chem. 269, 1583–1586.
[18] van Hoek, A.N., Hom, M.L., Luthjens, L.H., de Jong, M.D., Dempster, J.A. and van Os, C.H. (1991) J. Biol. Chem. 266, 16633–16635.
[19] Zhang, R., van Hoek, A.N., Biwersi, J. and Verkman, A.S. (1993) Biochemistry 32, 2938–2941.
[20] Preston, G.M., Jung, J.S., Guggino, W.B. and Agre, P. (1993) J. Biol. Chem. 268, 17–20.
[21] Shi, L.B., Skach, W.R. and Verkman, A.S. (1994) J. Biol. Chem. 269, 10417–10422.
[22] Engel, A., Walz, T. and Agre, P. (1994) Curr. Opin. Struct. Biol. 4, 545.
[23] Zeidel, M.L., Nielsen, S., Smith, B.L., Ambudkar, S.V., Maunsbach, A.B. and Agre, P. (1994) Biochemistry 33, 1606–1615.
[24] Cheng, A., van Hoek, A., Yeager, M., Verkmana, A. and Mitra, A. (1997) Nature 387, 627–630.
[25] Li, H., Lee, S. and Jap, B.K. (1997) Nat. Struct. Biol. 4, 263–265.
[26] Walz, T., Smith, B., Agre, P. and Engel, A. (1994) EMBO J. 13, 2985–2993.
[27] Walz, T. et al. (1997) Nature 387, 624–627.
[28] de Groot, B.L., Heymann, J.B., Engel, A., Mitsuoka, K., Fujiyoshi, Y. and Grubmuller, H. (2000) J. Mol. Biol. 300, 987–994.
[29] Brünger, A.T. (1992) X-PLOR, Version 3.1: A System for X-ray Crystallography and NMR, The Howard Hughes Medical Institute and Department of Molecular Biophysics and Biochemistry, Yale University.
[30] Zhang, L. and Hermans, J. (1996) Proteins Struct. Funct. Genet. 24, 433–438.
[31] Grubmuller, H. (1996) SOLVATE v. 1.0, Theoretical Biophysics Group, Institute for Medical Optics, Ludwig-Maximilians University, Munich.
[32] Heller, H., Schaefer, M. and Schulten, K. (1993) J. Phys. Chem. 97, 8343–8360.
[33] Gullingsrud, J., Kosztin, D. and Schulten, K. (2001) Biophys. J. 80, 2074–2081.
[34] Humphrey, W.F., Dalke, A. and Schulten, K. (1996) J. Mol. Graphics 14, 33–38.
[35] Insight II Version 98.0, Molecular Modeling System (1998) Molecular Simulations Inc., San Diego, CA.
[36] MacKerell Jr., A.D., Bashford, D., Bellott, M., Dunbrack Jr., R.L., Evanseck, J., Field, M.J., Fischer, S., Gao, J., Guo, H., Ha, S., Joseph, D., Kuchnir, L., Kuczera, K., Lau, F.T.K., Mattos, C., Michnick, S., Ngo, T., Nguyen, D.T., Prodhom, B., Roux, B., Schlenkrich, M., Smith, J., Stote, R., Straub, J., Watanabe, M., Wiorkiewicz-Kuczera, J., Yin, D. and Karplus, M. (1992) FASEB J. 6, A143.
[37] MacKerell Jr., A.D., Bashford, D., Bellott, M., Dunbrack Jr., R.L., Evanseck, J., Field, M.J., Fischer, S., Gao, J., Guo, H., Ha, S., Joseph, D., Kuchnir, L., Kuczera, K., Lau, F.T.K., Mat-

tos, C., Michnick, S., Ngo, T., Nguyen, D.T., Prodhom, B., Reiher, I.W.E., Roux, B., Schlenkrich, M., Smith, J., Stote, R., Straub, J., Watanabe, M., Wiorkiewicz-Kuczera, J., Yin, D. and Karplus, M. (1998) J. Phys. Chem. B 102, 3586–3616.
[38] Kalé, L., Skeel, R., Bhandarkar, M., Brunner, R., Gursoy, A., Krawetz, N., Phillips, J., Shinozaki, A., Varadarajan, K. and Schulten, K. (1999) J. Comp. Phys. 151, 283–312.
[39] Essmann, U., Perera, L., Berkowitz, M.L., Darden, T., Lee, H. and Pedersen, L.G. (1995) J. Chem. Phys. 103, 8577–8593.
[40] Sui, H., Walian, P.J., Tang, G., Oh, A. and Jap, B.K. (2000) Acta Crystallogr. D 56, 1198–1200.